ELSEVIER

Chemical Physics 255 (2000) 369–378

Chemical Physics

www.elsevier.nl/locate/chemphys

Photodissociation spectroscopy of ClCN in the vacuum ultraviolet region

Kazuhiro Kanda [a,*], Mitsuhiko Kono [b,1], Takashi Nagata [b,2], Atsunari Hiraya [b,3], Kiyohiko Tabayashi [b,4], Kosuke Shobatake [b,5]

[a] *Laboratory of Advanced Science and Technology for Industry, Himeji Institute of Technology, Kamigori, Hyogo 678-1205, Japan*
[b] *Institute for Molecular Science, Okazaki, Aichi 444-8585, Japan*

Received 21 February 2000

Abstract

The quantitative photofragment fluorescence spectroscopy, using the synchrotron radiation as an exciting light source, was applied to study the Rydberg and high-lying valence states of ClCN observed as congested structures in the vacuum ultraviolet region. The absolute cross-section and quantum yield for the CN($B\,^2\Sigma^+$–$X\,^2\Sigma^+$) emission produced in the photodissociation process of ClCN were determined in the wavelength range 105–145 nm (69 000–95 200 cm^{-1}). The quantum yield for the CN($B\,^2\Sigma^+$) production takes a maximum value of ≈0.13 at ≈84 000 cm^{-1}. The emission of CN($B\,^2\Sigma^+$–$X\,^2\Sigma^+$) transition was found to be partially polarized with respect to the direction of the electric vector of the excitation synchrotron radiation. The polarization anisotropy of this emission, which depends on the symmetry of absorption transitions into the photodissociative states of ClCN was measured as a function of exciting wavelength. The relative cross-section for the production of CN($A\,^2\Pi_i$–$X\,^2\Sigma^+$) emission was also determined. Based on the measured photochemical properties of the high-energy electronic states, the observed bands of the Rydberg and intravalence transitions are assigned.

1. Introduction

In the vacuum UV (VUV) photodissociation process of ClCN, the electronically excited radicals of CN($B\,^2\Sigma^+$) and CN($A\,^2\Pi_i$) are produced as the photofragments and the subsequent CN($B\,^2\Sigma^+$–$X\,^2\Sigma^+$) and CN($A\,^2\Pi_i$–$X\,^2\Sigma^+$) emissions have been observed in the UV and visible region and in the near infrared region, respectively. The knowledge of the high-lying electronic states is important to discuss the photodissociation dynamics of ClCN in the VUV region. However, the congested features of the VUV absorption spectrum of ClCN prevented us from the fully understanding the property of the precursor states, (ClCN)*, through

* Corresponding author.
[1] Present address: Solar-Terrestrial Environment Laboratory, Nagoya University, Toyokawa, Aichi 442-8507, Japan
[2] Present address: Department of Basic Science, Graduate School of Arts and Sciences, Meguro-ku, Tokyo 153-8902, Japan.
[3] Present address: Department of Material Science, Faculty of Science, Hiroshima University, Higashi-Hiroshima, Hiroshima 739-8526, Japan.
[4] Present address: Department of Chemistry, Graduate School of Science, Hiroshima University, Higashi-Hiroshima, Hiroshima 739-8526, Japan.
[5] Present address: Department of Materials Chemistry, School of Engineering, Nagoya University, Chikusa-ku, Nagoya 464-8603, Japan.

0301-0104/00/$ - see front matter
PII: S0301-0104(00)00064-1

which fragmentation proceeds. Although electronic excited states of ClCN have been investigated by several workers, their assignments are not all consistent and the peaks in the $\lambda < 120$ nm have not been assigned [1–7].

Through systematic work, we have investigated the highly excited states of the cyanogen halide leading to the production of CN(A) and CN(B) radicals. In our previous works, the transition peaks observed in the VUV absorption spectra of BrCN and ICN have been assigned to the Rydberg series and the intravalence transitions [8,9]. The same transitions are expected to appear in the photoabsorption spectrum of ClCN, because ClCN has the chemical properties similar to these molecules. On the other hand, the spectral positions must be shifted because the ionization potentials of ClCN are higher than those of BrCN and ICN.

In the present study, the absolute cross-section and quantum yield for the production of CN(B) in the VUV photodissociation process of ClCN were determined as a function of excitation wavelength ranging from 105 to 145 nm. In addition to these quantitative measurements, the polarization anisotropy of the resulting CN($B\,^2\Sigma^+$–$X\,^2\Sigma^+$) emission was measured by taking advantage of the linear polarization of the synchrotron radiation. The polarization anisotropy of the fragment emission with respect to the direction of the electric vector of incident radiation gave us an information on the symmetry of the initial electronic transition into the dissociative state. Measurements for the polarization anisotropy of CN(B–X) observed in the VUV photodissociation process of ClCN have been reported by Simons and coworkers at several excitation wavelengths in the 126–154 nm region [3,4] and by Zare and coworkers at 157.6 nm [10]. In the present experiment, the polarization anisotropy of CN(B–X) was measured as a function of wavelength ranging from 105 to 145 nm at intervals of 0.02 nm. Our "close" measurement distinguished the tiny structures in the excitation function from the underlying diffuse bands and made the spectral assignments of the VUV absorption bands of ClCN reliable. The relative cross-section for the CN(A) production in the VUV photodissociation process of ClCN was also measured.

2. Experimental

The experimental apparatus and procedures employed in the present study have been described in the previous paper [8,9,11]. The measurement was performed at the BL2A stage of UVSOR in the Institute for Molecular Science. The synchrotron radiation provided by the 0.75-GeV electron storage ring was dispersed by a 1-m Seya-Namioka monochromator (Hitachi SNM-2) and was introduced into the 12.3-cm-length reaction flow cell through the LiF window. Slit widths of the monochromator were 100 μm for the measurement of the absorption and fluorescence excitation spectra, and 300 μm for the measurement of the polarization anisotropy of CN(B–X) emission. These resolutions of exciting light wavelength were about 0.1 and 0.3 nm, respectively, which were estimated from the spectral width of the atomic absorption line of Kr at 123.6 nm and those of Xe at 119.20 and 146.96 nm. A wavelength reading of the monochromator was calibrated against these atomic absorption lines. The uncertainty in the calibrated wavelength was estimated to be ±0.03 nm.

The ClCN sample was prepared by the reaction of NaCN with Cl_2 in a CCl_4 medium at −10°C [12]. The pressure of sample in the reaction flow cell monitored with a capacitance manometer (Baratron Type 315) was typically 15–45 mTorr (1 Torr = 133.322 Pa). The VUV photons passing through the cell were detected by a Hamamatsu R585 photomultiplier after conversion to visible fluorescence by sodium salicylate coated on the outside of the exit LiF window. The output signal from the photomultiplier tube was fed into a picoammeter (TDA AM-271A). The photoabsorption cross-section, σ, was determined from the ratio of the VUV photon fluxes through the flow cell measured with and without sample gas. The uncertainty of the absolute absorption cross-section was estimated to be ≈10% due to the uncertainty of the sample gas pressure.

The fragment emissions were collimated through a quartz lens attached on the side wall of the reaction flow cell and focused through another quartz lens to a detector. The CN(B–X) emission in the UV and visible region was isolated by

a band-pass filter (Toshiba C-39A) and detected by a photomultiplier (Hamamatsu R585). The emission of CN(A–X) transition observed in the near infrared region was monitored with a combination of a sharp-cut filter (Toshiba R-65) and a photomultiplier (Hamamatsu R955) equipped with a photomultiplier cooler (Hamamatsu C659). The emission signal was acquired using an Ortec photon counting system. The emission cross-section determined in the present study corresponds to the cross-section for the production of CN(B), σ_B, because the radiative decay can be regarded as the dominant deexcitation process for the CN formed in the B state. The absolute value of σ_B was scaled by a comparison of the intensity of the CN(B–X) emission produced in the photodissociation of HCN, for which the absolute emission cross-section has been reported [13]. The details about the scaling procedure to obtain the absolute emission cross-section from the emission intensity and relative optical responses of the detection systems were described in Ref. [9]. The relative uncertainty of σ_B was estimated to be $\approx$10%. On the other hand, the absolute values of the cross-section for the production of CN(A), σ_A, could not be determined, because the detection system for the near infrared region did not cover all the spectral region of CN(A–X) transitions, as discussed in Ref. [9]. The quantum yield for the production of CN(B), Γ_B, was calculated as the ratio of the emission cross-section to the absorption cross-section. The relative uncertainty of Γ_B was estimated to be $\approx$20%.

The polarization anisotropy, R, is defined as

$$R = (I_\parallel/I_\perp - 1)/(I_\parallel/I_\perp + 2), \quad (1)$$

where $I_\parallel$ and $I_\perp$ are the intensities of the emission with the light component parallel and perpendicular to the direction of the electric vector of the incident radiation, respectively. In order to measure the polarization anisotropy of CN(B–X) emission produced in the photodissociation process of ClCN, two identical sets of a band-pass filter and a Glan-Taylor prism polarizer (Karl–Lambrecht MGTYA15) were mounted behind the collimating quartz lenses [8]. The absolute values of the $I_\parallel/I_\perp$ ratio for the CN(B–X) emission were determined by using a photoelastic modulator (PEM, Hinds International Inc. PEM-80) and a multichannel scaler (MCS) at several excitation wavelengths, in order to eliminate the factors giving rise to the uneven signal levels of $I_\parallel$ and $I_\perp$. The details in the PEM–MCS technique have been described in Ref. [11]. The statistical errors in the measurement of the $I_\parallel/I_\perp$ ratio gave rise to the uncertainty of $\sim$0.01 of R.

3. Results and discussion

3.1. Electronic structure of cyanogen chloride

The molecular orbital (MO) configuration of ClCN in the ground state is given in the following [14–16]:

$$(1\sigma)^2(2\sigma)^2(3\sigma)^2(1\pi)^4(4\sigma)^2(2\pi)^4; \quad {}^1\Sigma^+ \quad (2)$$

The ionization potentials, IP, the frequencies of the vibrational modes, ν_1, ν_2, and ν_3 and spin–orbit splittings, SO, are listed in Table 1. The three band systems are observed in the photoelectron spectrum of cyanogen chloride. The cyanogen chloride cations in these three lowest energy ionic states and the cyanogen chloride in the ground state have been reported to be linear [14–17].

The first band system (IP = 99 770 cm^{-1}) in the photoelectron spectrum are due to the removal of an electron from the 2π MO, which originates from the combination of the 3p orbital of the chlorine atom and the π bonding orbital of the CN group out of phase. The splitting of this band system by spin–orbit coupling, i.e. the splitting between $ClCN^+(X\,^2\Pi_{3/2})$ and $ClCN^+(X\,^2\Pi_{1/2})$, is small in comparison with BrCN and ICN. The photoelectron intensity of the $X\,^2\Pi_{3/2}$ component is much smaller than that of the $X\,^2\Pi_{1/2}$ component. The second band system (IP = 111 300 cm^{-1}) is due to ionization of cyanogen chloride to the $^2\Sigma^+$ state, which corresponds to the removal of an electron from the 4σ MO. The 4σ orbital is regarded primarily as the lone pair localized on the nitrogen atom. The third band system (IP = 124 000 cm^{-1}) arises from the removal of an electron from the 1π MO. This MO is the combination

Table 1
Ionization potentials, vibrational frequencies and spin–orbit splittings (cm^{-1})

State	IP	Vibrational frequencies[a]			SO
		ν_1	ν_2	ν_3	
ClCN					
$X\,^1\Sigma^+$	0	714.02[b]	378.62[b]	2215.24[b]	
$ClCN^+$					
$(2\pi)^{-1}$, $X\,^2\Pi_{3/2}$	99 770[c]	827[d]	376[d]	1915[d]	
					276[d]
$(2\pi)^{-1}$, $X\,^2\Pi_{1/2}$		829[d]		1914[d]	
$(4\sigma)^{-1}$, $A\,^2\Sigma^+$	111 300[c]	774[d]	545[d]		
$(1\pi)^{-1}$, $B\,^2\Pi_{3/2}$	124 000[c]	531.8[d]	303.1[d]	2128.5[d]	
					368[d]
$(1\pi)^{-1}$, $B\,^2\Pi_{1/2}$		529.7[d]			

[a] ν_1: C–N stretching, ν_2: bending, ν_3: C–Cl stretching.
[b] Ref. [17].
[c] Ref. [14].
[d] Ref. [20].

of the 3p orbital of the chlorine atom and the π bonding orbital of the CN group in phase.

3.2. Absorption and excitation spectra

Fig. 1 shows the VUV absorption spectrum of ClCN in the 69 000–95 200 cm^{-1} region. The spectral features and positions of the absorption bands observed in the present study are in good agreement with the photoabsorption spectrum of ClCN, which has been previously reported by Simons et al. [3,4] and Felps et al. [5,7].

In Fig. 2(a), the absolute cross-section and quantum yield for the CN(B) production are plotted against the excitation wave number, $\tilde{\nu}$, in the range 69 000–95 200 cm^{-1}. The excitation spectrum of CN(B–X) emission formed from the VUV photodissociation of ClCN has been reported previously by Macpherson and Simons [3,4] in the region $\tilde{\nu} < 81\,900$ cm^{-1} (122 nm) while the absolute cross-section of the CN(B–X) emission has not been determined in their studies. The dominant photodissociation channels in the 69 000–95 200 cm^{-1} region lead to the production of CN fragments in the X and/or A states, because the observed maximum value of Γ_B is only ≈0.13 at ≈84 000 cm^{-1}.

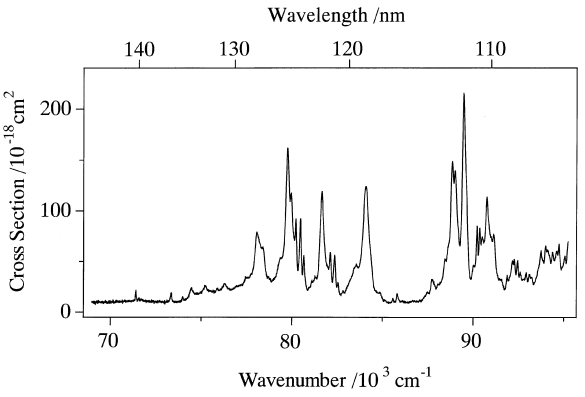

Fig. 1. Photoabsorption cross-section of ClCN in the 69 000–95 200 cm^{-1} range. The spectral resolution is ≈0.1 nm.

Fig. 2(b) depicts the polarization anisotropy, R, of the subsequent CN(B–X) emission as a function of the excitation wave number. The values of R expected in the photodissociation of cyanogen halide have been discussed in Ref. [8]. By considering the fact that ClCN is a linear molecule and that the transition dipole moment responsible for the fragment CN($B\,^2\Sigma^+$–$X\,^2\Sigma^+$) emission is fixed along the molecular axis of the CN fragment, the limiting value of R merely depends on the type of absorption transitions relevant to the photodissociation of ClCN. In the case of parallel-type transition, when the transition dipole moment for the absorption of ClCN, μ_{abs}, is parallel with the molecular axis, i.e., μ_{abs} is perpendicular to the angular momentum, J, theoretical limit of R value is calculated to be 0.1. On the other hand, when μ_{abs} is perpendicular to

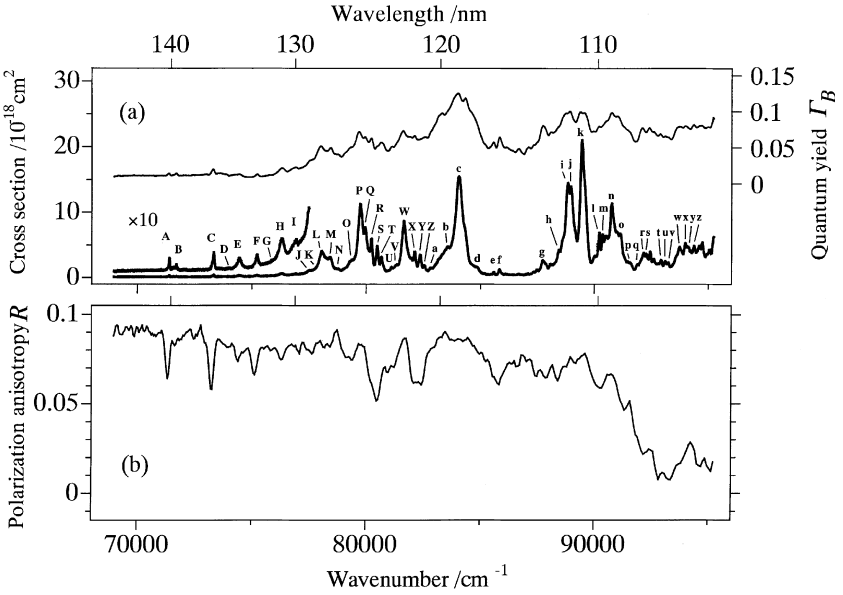

Fig. 2. (a) Absolute cross-section (—) and quantum yield (—) for the production of CN($B\,^2\Sigma^+$) from ClCN in the 69 000–94 000 cm^{-1} range. (b) Polarization anisotropies of CN($B\,^2\Sigma^+$–$X\,^2\Sigma^+$) emission.

the molecular axis (perpendicular-type transition), i.e. $\mu_{abs} \| J$, the R value will be 0.1 and −0.2 in the P and R branches and in the Q branch, respectively. In a predissociation process, the observed magnitude of R is reduced to be less than these theoretical limit by the rotational motions of the dissociating [ClCN*] molecule during its lifetime. Simons et al. have measured the $I_{\|}/I_{\perp}$ ratio of the CN(B–X) emission from ClCN at several excitation wavelengths [3,4]. The R values measured in the present study at the corresponding wavelengths agree well with those previously reported values [3,4] within the experimental accuracy.

Fig. 3 shows the excitation spectrum and relative quantum yield for the CN($A^2\Pi_i$) production in the wave number region 69 000–95 200 cm^{-1}. The wave number dependence of the cross-section for the CN(A) production resembles that for the CN(B) production in this region.

3.3. Spectral assignments

The photoabsorption peaks observed in the present measurement were interpreted in terms of excitations to the valence excited states and the Rydberg states. The transition frequency, $\tilde{\nu}$, of a Rydberg series obeys the formula

$$\tilde{\nu} = \mathrm{IP} - \frac{R_\infty}{(n-\delta)^2}, \tag{3}$$

where R_∞ represents the Rydberg constant (10 973 cm^{-1}) and n is the principal quantum number. The quantum defect, δ, is characteristic of a given Rydberg series, however, no regular Rydberg series are expected to appear in the photoabsorption spectra of cyanogen halide due to strong interaction between intravalence and Rydberg states [8,9]. In the following sections, we discuss the assignments of the photoabsorption peaks and photochemical properties of the excited states on the basis of the measurements of the excitation spectra and polarization anisotropy.

3.3.1. $2\pi \rightarrow ns\sigma$ Rydberg transition

The absorption bands observed in the 71 000–78 000 cm^{-1} region have been assigned to the leading members of the $2\pi \rightarrow ns\sigma$ Rydberg series by Felps and co-workers [5–7]. The vibrational structures are characteristic of a linear–linear transition of triatomic molecule, i.e. the vibrational

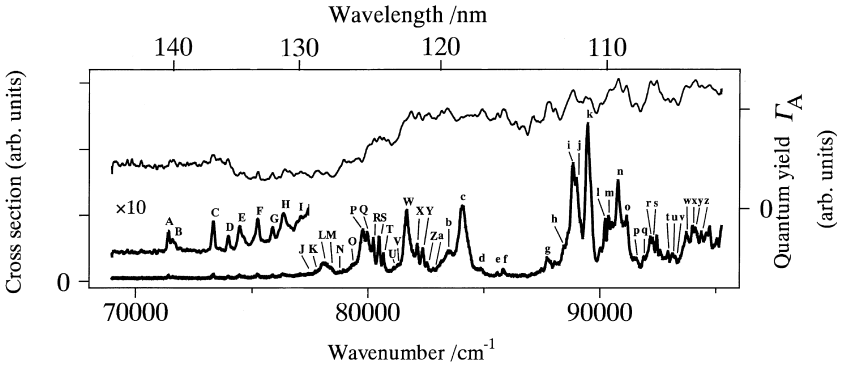

Fig. 3. Relative cross-section (—) and quantum yield (—) for the production of CN(A $^2\Pi_i$) from ClCN in the 69 000–94 000 cm^{-1} range.

band associated with the v_2 mode (bending vibration) was not observed except for very weak 71 705 cm^{-1} band. The fragment CN(B–X) emission intrinsically processes negative polarization because a sharp dip is observed at the center of the intense absorption peaks in this region of the R–$\tilde{\nu}$ curve. This indicates that the photoexcitation at the band center results in a negative R value of the CN(B–X) emission. The dependence of polarization on $\tilde{\nu}$ is characteristic of the Q branch excitation of a perpendicular-type transition of ClCN [18]. The quantum defect for band origin at 71 398 cm^{-1} with respect to the first ionization potential is calculated to be 1.03.

The baseline of the excitation spectra is not zero, which is ascribable to the contribution of an underlying continuum. The R value takes ≈0.09 in the excitation energy region, where the underlying continuum makes a dominant contribution to the production of CN(B). The positive R value indicates that the photoexcitation responsible for the CN(B) production occurs through a parallel-type transition of ClCN [18]. This underlying continuum is assignable to the high-energy tail of the α continuum (the $2\pi \rightarrow 3\pi$ intravalence excitation), which extends over 62 000–70 600 cm^{-1} [7]. The large magnitude of R, which is close to the limiting value, 0.1, is also consistent with the operation occurrence of direct photodissociation via the α continuum. A non-zero Γ_B above 71 000 cm^{-1} obviously conflicts with the semiquantitative prediction based on a simple one-electron MO model that the threshold energy for the Cl + CN(B) channel is predicted to locate at 110 140 cm^{-1} [7]. The vibrational analysis of this band system is listed in Table 2.

The peak at 85 822 cm^{-1} (f) is accompanied with v_3 and $v_1 + v_3$ vibrational bands at 87 750 (g) and 88 449 cm^{-1} (h). These structures of vibrational progression resemble those of peaks (A), (C) and (D). Dips in the R–$\tilde{\nu}$ curve show that perpendicular-type transition is responsible for this band system. Therefore, this band system is assignable to the $2\pi \rightarrow 4s\sigma(^1\Pi)$ Rydberg transition. The band origin of the $2\pi \rightarrow 5s\sigma(^1\Pi)$ Rydberg transition is assigned to the peak at 92 268 cm^{-1} (s).

3.3.2. $2\pi \rightarrow 6\sigma$ intravalence transition

In the energy range 74 000–77 000 cm^{-1}, another vibrational progressions (E, H and I) appear in the photoexcitation spectrum of ClCN. Because these bandwidths are clearly wider than near Rydberg bands i.e. $2\pi \rightarrow 3s\sigma$, the dissociation dynamics through these electronic states should be different from the Rydberg states. Felps et al. have assigned these peaks to the $2\pi \rightarrow 6\sigma(^1\Pi)$ intravalence transition [7]. These peaks are considered to arise from a perpendicular-type transition because the R–$\tilde{\nu}$ curve shows a minimum at the center of these peaks. Our experimental result reinforces their assignments. The present vibrational analysis of this band system is shown in Table 3.

Table 2
Wave numbers/wavelengths and assignments of Rydberg transitions in the vacuum UV absorption spectrum of ClCN

Peak[a]	$\tilde{\nu}$ (cm^{-1})[b]	λ (nm)[c]	$\Delta\tilde{\nu}$ (cm^{-1})[d]	n	Assignment	δ[e]
$2\pi \rightarrow n s\sigma(^1\Pi)$						
A	71 398	140.06		3	0_0^0	1.03
B	71 705	139.46	307		2^1	
C	73 346	136.38	1948		3^1	
D	73 975	135.18	629		$1^1 3^1$	
F	75 233	132.94	1887		3^2	
G	75 884	131.78	651		$1^1 3^2$	
f	85 822	116.52		4	0_0^0	1.20
g	87 750	113.96	1928		3^1	
h	88 449	113.06	699		$1^1 3^1$	
m	90 367	110.66	1918		$1^1 3^2$	
s	92 268	108.38		5	0_0^0	1.18
t	92 937	107.60	669		1^1	
y	94 091	106.28	1823		3^1	
$2\pi \rightarrow n p\pi(^1\Sigma^+)$						
P	79 745	125.40		3	0_0^0	0.66
W	81 673	122.44	1928		3^1	
b	83 556	119.68	1883		3^2	
j	88 984	112.38		4	0_0^0	(triplet)
k	89 445	111.80		4	0_0^0	0.74
l	90 204	110.86	759		1^1	
p	91 458	109.34	2013		3^1	
r	92 166	108.50	708		$1^1 3^1$	
x	93 985	106.40	1819		$1^1 3^2$	
w	93 738	106.68		5	0_0^0	0.74
z	94 357	106.28	619		1^1	
$2\pi \rightarrow n d\sigma(^1\Pi)$[f]						
o	91 125	109.74		4	0_0^0	0.44
q	91 878	108.84	753		1^1	
u	93 127	107.38	2002		3^1	
$4\sigma \rightarrow n s\sigma(^1\Sigma^+)$						
c	84 076	118.94		3	0_0^0	0.99
d	84 846	117.86	770		1^1	
e	85 587	116.84	741		1^2	
$4\sigma \rightarrow n p\sigma(^1\Sigma^+)$						
i	88 842	112.56		3	0_0^0	0.79
n	90 761	110.18	1919		3^1	

[a] The symbols correspond to those in Figs. 2 and 3.
[b] Errors in $\tilde{\nu}$ are estimated to be ± 25 cm^{-1}.
[c] Errors in λ are estimated to be ± 0.03 nm.
[d] Frequency interval for the vibrational progressions. These values are comparable to the wave numbers of the corresponding ν_1, ν_2 and ν_3 modes of $ClCN^+$ (see Table 1).
[e] Quantum defect.

3.3.3. $2\pi \rightarrow 4\pi$ intravalence transition

The band structures observed at $\approx$78 000 cm^{-1} in the photoexcitation spectrum are too diffuse to identify their band origins and vibrational progressions. Macpherson and Simons have assigned these bands to the $^3\Pi$ and $^1\Pi$ manifolds arising from the $2\pi \rightarrow 3p\sigma$ Rydberg transition [3]. Felps et al. have mentioned this band system only due to Rydberg transitions [7]. The positive R, $\approx$0.09, which is close to the theoretical limit for direct

Table 3
Wave numbers/wavelengths and assignments of the intravalence transitions in the vacuum UV absorption spectrum of ClCN[a]

Peak	$\tilde{\nu}$ (cm^{-1})	λ (nm)	$\Delta\tilde{\nu}$ (cm^{-1})	Assignment
$2\pi \rightarrow 6\sigma(^1\Pi)$				
E	74 471	134.30		0_0^0
H	76 301	131.06	1830	3^1
I	76 959	129.94	658	$1^1 3^1$
$2\pi \rightarrow 4\pi(^1\Sigma^+)$[b]				
J	77 459	129.10		0_0^0
K	77 761	128.60	302	1^1
L	78 064	128.10	303	1^2
M	78 395	127.56	331	1^3
N	78 715	127.04	320	1^4
O	79 340	126.04	625	1^6
Q	79 962	125.06	622	1^8
$1\pi \rightarrow 5\sigma(^1\Pi)$				
R	80 218	124.66		0_0^0
S	80 476	124.26	258	2^1
T	80 658	123.98	182	2^2
U	81 116	123.28	640	$1^1 2^1$
V	81 288	123.02	172	$1^1 2^2$
X	82 129	121.76	1911	3^1
Y	82 359	121.42	230	$2^1 3^1$
Z	82 549	121.14	190	$2^2 3^1$
a	82 823	120.74	694	$1^1 3^1$

[a] See legend of Table 2.
[b] Tentative assignments (see text).

dissociation values, indicates that a parallel-type transition makes a dominant contribution to these band structures. It is concluded from this observation that the relevant upper state is dissociative and that its lifetime is much shorter than the rotational period of ClCN. This band system is tentatively assigned to the $2\pi \rightarrow 4\pi(^1\Sigma^+)$ intravalence transition, which was also observed in the photoabsorption spectrum of ICN as discussed in Ref. [9]. The vibrational analysis of this band system is listed in Table 3.

3.3.4. $2\pi \rightarrow np\pi$ Rydberg transition

The most intense absorption band peaking at 79 745 cm^{-1} has been assigned to the $2\pi \rightarrow 3p\pi$ Rydberg transition by Macpherson and Simons [3]. As shown in Fig. 2(b), the R–$\tilde{\nu}$ curve shows a maximum at the center of the intense absorption peak located at 79 745 cm^{-1} (P). This implies that a parallel-type transition is responsible for this peak. The R–$\tilde{\nu}$ curve also shows humps at 81 673 (W) and 83 556 (b) cm^{-1} peaks, which are assignable to the vibrational members of the ν_3 progressions. Based on these findings, this band system is associated with the $2\pi \rightarrow 3p\pi(^1\Sigma^+)$ transition. Our present result supports the assignment by Macpherson and Simons [3]. The $n = 4$ and $n = 5$ members of this transition are observed at 89 445 cm^{-1} (k) and 93 738 cm^{-1} (w), respectively, as listed in Table 2.

3.3.5. $1\pi \rightarrow 5\sigma$ intravalence transition

In the energy range 80 200–81 300 cm^{-1}, several peaks appear in the photoabsorption spectrum of ClCN. Macpherson et al. and Felps et al. have assigned these peaks to the $4\sigma \rightarrow 3s\sigma$ and $2\pi \rightarrow 3p\pi$ Rydberg transitions, respectively [3,7]. However, dips at the center of the absorption peaks are observed in the R–$\tilde{\nu}$ curve. The dips are also observed at $\approx$82 100 cm^{-1}, corresponding to the ν_3 excitation. Felps et al. have estimated the transition energy of the $1\pi \rightarrow 5\sigma$ intravalence transition to be $\approx$80 460 cm^{-1} [7]. Based on these observations, this band system is assigned to the $1\pi \rightarrow 5\sigma(^1\Pi)$ intravalence transition. The molecular structure of this excited state is presumably bent, because the ν_2 (bending vibration) mode progressions were observed. The molecular bond angle could be changed from 180° by the strong Renner–Teller effect due to the $^1\Pi$ type intravalence electronic state. The spectral position of band origin is not obvious. The tentative vibrational analysis of this band system is listed in Table 3.

3.3.6. $4\sigma \rightarrow ns\sigma$ Rydberg transition

The band at 84 076 cm^{-1} (c) is accompanied with ν_1 and $2\nu_1$ vibrational bands at 84 846 (d) and 85 587 cm^{-1} (e), respectively. The positive R values indicate that parallel-type transition makes a dominant contribution to this band system. The quantum defect for the band origin at 84 076 cm^{-1} with respect to the second ionization potential (113 000 cm^{-1} [14]) is calculated to be 0.99; an electron promotion to an s-type Rydberg orbital is involved in the transition [19]. Based on these considerations, this band system is assigned to the $4\sigma \rightarrow 3s\sigma(^1\Sigma^+)$ Rydberg transition (see Table 2).

This band has the highest quantum yield for the production of CN(B) in the present observed region. The promotion of the 4σ electron preferentially leads to the production of CN(B), from the molecular orbital correlation between parent ClCN and CN(B) fragment.

3.3.7. $4\sigma \rightarrow np\sigma$ Rydberg transition

The peak located at 88 842 cm^{-1} (i) is assigned to the band origin of the $4\sigma \rightarrow 3p\sigma(^1\Sigma^+)$ Rydberg transition because the quantum defect for the origin with respect to the second ionization potential is calculated to be 0.79, which accords with an electron promotion to a p-type Rydberg orbital [19]. The R–$\tilde{\nu}$ curve shows a small hump at 90 761 cm^{-1} (n) peak, which is assignable to the vibration member of the ν_3 progression.

3.3.8. $2\pi \rightarrow nd\sigma$ Rydberg transition

The type of absorption transition responsible for the 91 125 cm^{-1} peak (o) cannot be determined definitely from R value, due to the intense neighboring 90 761 cm^{-1} peak (n), which is assigned to the 3^1 band of the $4\sigma \rightarrow 3p\sigma$ transition. This band is assignable to the $2\pi \rightarrow 4d\sigma(^1\Pi)$ transition from a quantum defect $\delta \approx 0.44$. The 91 878 (q) and 93 127 (u) cm^{-1} peaks are assignable to the vibrational members of the ν_1 and ν_3 progression, respectively (see Table 2).

4. Conclusions

The high-energy lying states of ClCN was investigated by the measurement of the excitation spectra and the polarization anisotropy of relevant fluorescence by taking advantage of the linear polarization of synchrotron radiation. Almost dominant absorption bands in the wavelength range 105–145 nm were assigned on the basis of the symmetry of the upper electronic state. The $2\pi \rightarrow 4\pi$, $1\pi \rightarrow 5\sigma$ intravalence transitions and $4\sigma \rightarrow ns\sigma$, $4\sigma \rightarrow np\sigma$ and $2\pi \rightarrow nd\sigma$ Rydberg series were assigned first in the present study. Higher members of the $2\pi \rightarrow ns\sigma$, $2\pi \rightarrow np\pi$ Rydberg series could be assigned up. The transitions observed in the photoabsorption spectrum of ClCN are consistent with those observed in the photoabsorption of BrCN and ICN, however, the $^3\Pi$ manifold was not observed.

Rydberg transitions observed in the present study are converging to the first or second IPs of ClCN. These IPs exhibit in the shorter wavelength region than the present measurement range. We have measured the photoexcited spectra of cyanogen halides in the 30–105 nm by using the gas-filter apparatus. We will report the assignments and the chemical properties of the high-energy excited states of cyanogen halides in the forthcoming publication.

Acknowledgements

This work was supported by the Joint Studies Program of the Institute for Molecular Science. K.K. thanks Professor S. Matsui and Dr. Y. Haruyama for their interest and encouragement in the present study.

References

[1] G.W. King, A.W. Richardson, J. Mol. Spectrosc. 21 (1966) 339.
[2] G.W. King, A.W. Richardson, J. Mol. Spectrosc. 21 (1966) 353.
[3] M.T. Macpherson, J.P. Simons, J. Chem. Soc. Faraday Trans. II 75 (1979) 1572.
[4] M.N.R. Ashfold, A.S. Georgiou, A.M. Quinton, J.P. Simons, J. Chem. Soc. Faraday Trans. II 77 (1981) 259.
[5] W.S. Felps, S.P. McGlynn, G.L. Findley, J. Mol. Spectrosc. 86 (1981) 71.
[6] S.P. McGlynn, W.S. Felps, G.L. Findley, Chem. Phys. Lett. 78 (1981) 89.
[7] W.S. Felps, K. Rupnik, S.P. McGlynn, J. Phys. Chem. 95 (1991) 639.
[8] K. Kanda, S. Katsumata, T. Nagata, Y. Ozaki, T. Kondow, K. Kuchitsu, A. Hiraya, K. Shobatake, Chem. Phys. 175 (1993) 399.
[9] K. Kanda, S. Katsumata, T. Nagata, T. Kondow, A. Hiraya, K. Tabayashi, K. Shobatake, Chem. Phys. 218 (1997) 199.
[10] J.A. Guest, M.A. O'Halloran, R.N. Zare, Chem. Phys. Lett. 103 (1984) 261.
[11] M. Kono, K. Shobatake, J. Chem. Phys. 102 (1995) 5966.
[12] W.C. Fernelius, Inorganic Syntheses, vol. 2, McGraw-Hill, New York, 1946.
[13] L.C. Lee, Chem. Phys. 72 (1980) 6414.

[14] E. Heilbronner, V. Hornung, K.A. Muszkat, Helv. Chim. Acta 53 (1970) 347.
[15] R.F. Lake, H. Thompson, Proc. Roy. Soc. A 317 (1970) 187.
[16] J.M. Hollas, T.A. Sutherley, Mol. Phys. 22 (1971) 213.
[17] D.H. Whiffen, Spectrochim. Acta 34A (1978) 1173.
[18] M.T. Macpherson, J.P. Simons, R.N. Zare, Mol. Phys. 38 (1979) 2049.
[19] A.B.F. Duncan, Rydberg Series in Atoms and Molecules, Academic Press, New York, 1971.
[20] F.G. Celii, J. Fulara, J.P. Maier, M. Rösslein, Chem. Phys. Lett. 131 (1986) 325.